

MARS PATHFINDER ATMOSPHERIC ENTRY TRAJECTORY DESIGN

David A. Spencer[†] and Robert D. Braun^{*}

The Mars Pathfinder spacecraft will enter the Martian atmosphere directly from the interplanetary trajectory, at a relatively high velocity. The design of the nominal entry trajectory, and the accurate determination of potential trajectory dispersions, is necessary for the development of the Pathfinder Entry, Descent, and Landing (EDL) System.

Monte Carlo simulations have been developed, in order to quantify the range of possible entry trajectories and attitude profiles. The simulation results have impacted the entry system design, and have validated the EDL timeline.

INTRODUCTION

The primary objective of the Mars Pathfinder mission is to demonstrate a low-cost, reliable system for entering the Martian atmosphere and placing a lander safely on the surface of Mars. The Entry, Descent, and Landing (EDL) System is designed to accommodate the range of off-nominal entry trajectories that may occur due to uncertainties in navigational accuracy, atmospheric density, entry body and parachute drag profiles, parachute deployment timing, and landing site elevation. The design of the entry trajectory, along with the accurate determination of potential trajectory dispersions, is critical to the success of the Pathfinder mission.

Monte Carlo simulations have been developed, **in order to obtain** statistical information on conditions at significant points during the Pathfinder descent. The results of the Monte Carlo simulations have directly impacted the design of the Pathfinder **Aeroshell** Thermal Protection System¹, and have been used to design and validate the parachute deployment algorithm. Also, the size and orientation of the landing ellipse on the Mars surface has been determined.

[†] Member of Technical Staff, Navigation and Flight **Mechanics** Section, Jet Propulsion Laboratory, California Institute of Technology, Pasadena, California. Member AIAA.

^{*} Aerospace Engineer, Space Systems and Concepts Division, NASA Langley Research Center, Langley, Virginia. Member AIAA.

The Pathfinder spacecraft will enter the Martian atmosphere directly from the Earth-to-Mars interplanetary transfer trajectory, along a Mars-centered approach hyperbola. The entry vehicle will reach the atmospheric interface point (defined at a radius of 3522.2 km) with an inertial velocity of up to 7.35 km/s. The pathfinder trajectory approach is in contrast to that of the Viking Landers; the Viking spacecraft entered orbit about Mars, and imaged the planet surface for one month prior to entry, in order to find suitable landing sites. The Viking spacecraft entered the atmosphere with inertial velocities of roughly 4.5 km/s. The Viking Landers employed an active control system during the descent phase, and made soft landings on the Mars surface⁴. Pathfinder will not use active control during entry, but will rely upon a system of solid rockets and airbags to decelerate and buffer the spacecraft at landing. The Pathfinder EDL sequence of events is shown in Figure 1. Thirty minutes prior to atmospheric entry, the cruise stage will be jettisoned. The entry vehicle will enter the Mars atmosphere,

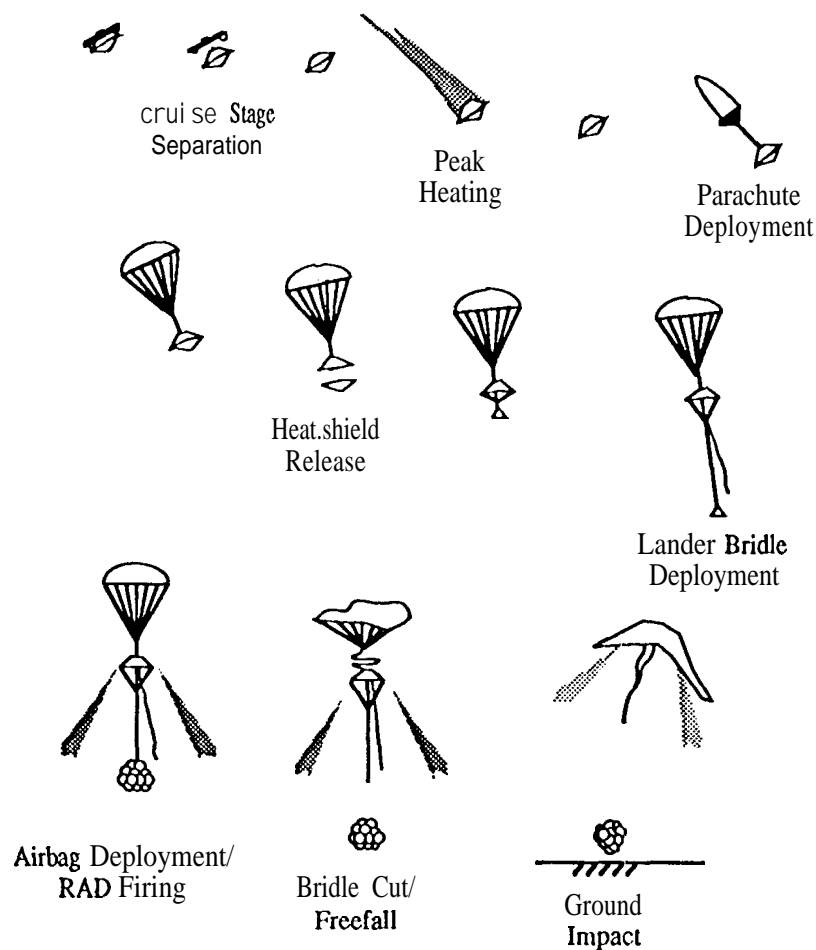


Figure 1. Entry, Descent and Landing Sequence of Events

reaching maximum stagnation point heating and **peak** dynamic pressure **during** the initial 70 seconds of the entry phase. At 162 seconds past **entry**, **a parachute will** redeployed, followed by the release of the heatshield 20 seconds later. The lander will be deployed below the **backshell** along a 20 m bridle. At an altitude of 1.5 km above ground level (AGL), a radar altimeter will acquire the ground. Altimeter data will **be used by the** flight software to inflate an airbag system and fire a set of three solid rockets (mounted on the **backshell**) at an altitude of 50 m AGL. At an altitude of 15 m, the bridle will be cut, and the lander will fall directly, buffered at ground impact by the airbag system. Sufficient impulse will remain in the solid rockets to carry the **backshell** and parachute to a safe distance away from the lander.

The Pathfinder target landing site is located at the outflow of a catastrophic flood system in the Ares Vanes region^s at **19.5°N, 32.8°W**. It is expected that this region will contain samples of a wide variety of Martian surface materials.

ENTRY TRAJECTORY REQUIREMENTS AND CONSTRAINTS

The Mars Pathfinder atmospheric entry trajectory is designed to fit within an envelope of derived requirements and physical constraints. **The primary design parameter that is varied to keep the 3 σ range of entry trajectories within the required envelope is the entry flight path angle, defined as the angle between the inertial velocity vector and the local horizontal at the atmospheric interface point, negative toward the planet. The entry flight path angle is bounded on the low, or shallow, end by the physical skipout angle constraint and the derived requirement on total integrated stagnation point heating. The 3 σ high (steep) entry flight path angle is bounded by the physical stagnation point pressure constraint of the aeroshell ablative material.**

For the Pathfinder mass and entry velocity, the limiting flight path angle for **skipout** from the Mars atmosphere is -11.2° (i.e., if the spacecraft inertial velocity vector is less than 11.2° below the local horizontal at the time of entry, **skipout** is predicted to occur). The Pathfinder Project has required that the entry trajectory be designed so that the worst-case inertial flight path angle at entry is at least 2° steeper than the skipout angle.

Arc-jet testing at NASA Ames **Research Center** has demonstrated that the **aeroshell** ablative material (**SLA-561 V**) can maintain its physical integrity at stagnation point pressures of 25.332kPa (0.25 Earth atm) **or less**⁶. At stagnation point pressures greater than **25.332 kPa**, surface **spallation** of the **aeroshell** ablative material can occur, effectively changing the aerodynamic characteristics of the **aeroshell** and creating uncertain heating conditions.

The EDL system will employ a Dacron supersonic parachute. The required parachute deployment conditions are as follows: dynamic pressure no greater than 703 Pa, Mach number greater than 1.2 and less than 2.3, and time from parachute deployment to 1.5 km AGL (earliest possible ground acquisition by the altimeter) greater than 55 s. This 55 s requirement allows sufficient time, including margin, for parachute stabilization, release of the **heatshield**, and lander deployment along the 20 m bridle.

The 3σ Pathfinder landing ellipse on the surface of Mars is required to be 100 x 270 km, centered on the coordinates 19.5°N, 32.8°W.

PARACHUTE DEPLOYMENT ALGORITHM

The Mars Pathfinder primary parachute deployment algorithm is based upon accelerometer measurements and a predetermined entry acceleration profile⁸. The algorithm is tuned specifically to the Pathfinder entry trajectory, for a ballistic coefficient of 65 kg/m² and a nominal inertial entry angle of -14.2°. An on-board timer is initiated when the sensed acceleration during atmospheric entry increases to five Earth g's (49.0 m/s²). Ten seconds after timer initiation, the acceleration is measured once again--based upon this sensed acceleration at 5 g + 10 seconds, a stored curve fit is consulted to determine the time of parachute deployment. The curve fit, shown in Figure 2, is a linear least-squares approximation to a series of data points derived by propagating entry trajectories of various flight path angles to a targeted dynamic pressure of 600 N/m². This target dynamic pressure was determined iteratively using Monte Carlo simulations, in order to satisfy the 3σ high parachute deployment dynamic pressure requirement of 703 N/m², while allowing the parachute to open at a sufficiently high altitude to allow the EDL sequence of events to occur. The Pathfinder parachute deployment algorithm has been implemented in the Monte Carlo simulations. Within the simulations, uncertainties are included for the accelerometer measurements (± 4.9 m/s², 3σ) and time measurements (± 0.25 s, 3σ).

On-board fault protection determines the validity of the accelerometer measurements. If it is determined that the measured accelerations are invalid during the primary opportunity, a backup opportunity will be implemented. This backup algorithm is designed in a similar manner to the primary, but in the decreasing portion of the acceleration curve during entry, seen in Figure 3. The on-board timer is initiated at 12 Earth g's (117.6 m/s²), and the time to parachute deployment is determined based upon a curve fit for acceleration values at the 12 g+ 15 seconds point. This overall parachute deployment algorithm is designed to insure that a 30 second computer brown-out can occur during entry without negating the probability of a successful parachute deployment.

In the case of accelerometer failure during entry, a secondary backup method of deploying the parachute has been developed. Based upon orbit knowledge following the final trajectory correction maneuver, it is possible to specify a fixed time (in terms of Coordinated Universal Time or Ephemeris Time) at which the parachute can be safely opened. As additional tracking data is received while the spacecraft nears Mars, the navigation estimate of the atmospheric entry time becomes increasingly accurate, and the probability of success of the fixed-time approach increases. Monte Carlo results indicate that the fixed-time approach provides greater than an eighty percent likelihood that the parachute will be deployed within the required conditions, based upon tracking data at five days prior to entry. In the final day prior to entry, this likelihood increases to over ninety percent.

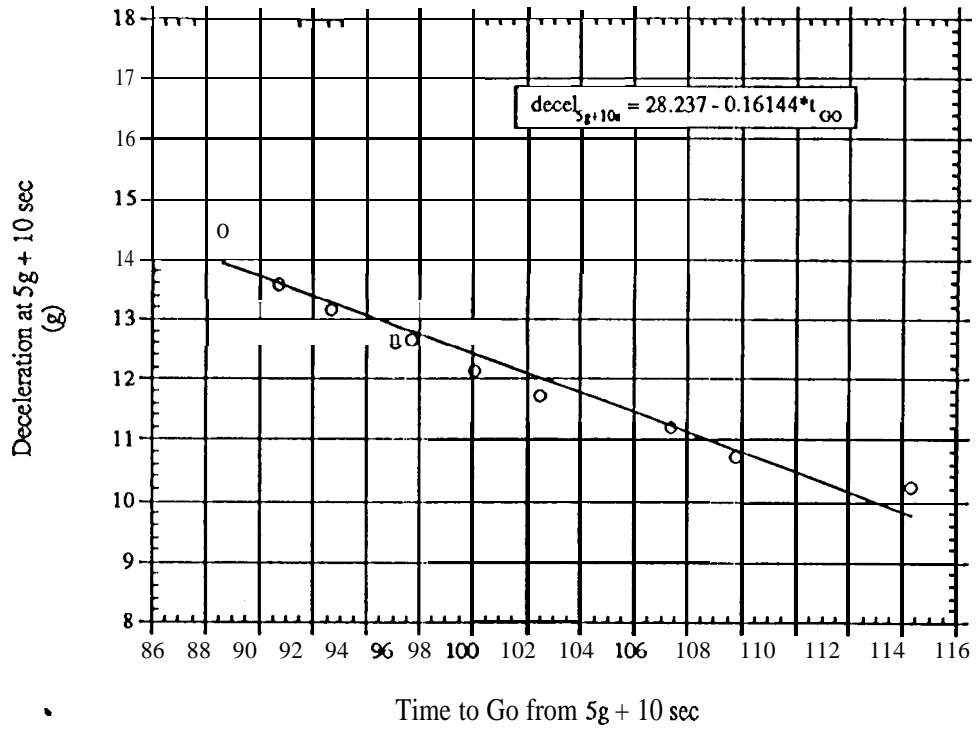


Figure 2. Parachute Deployment

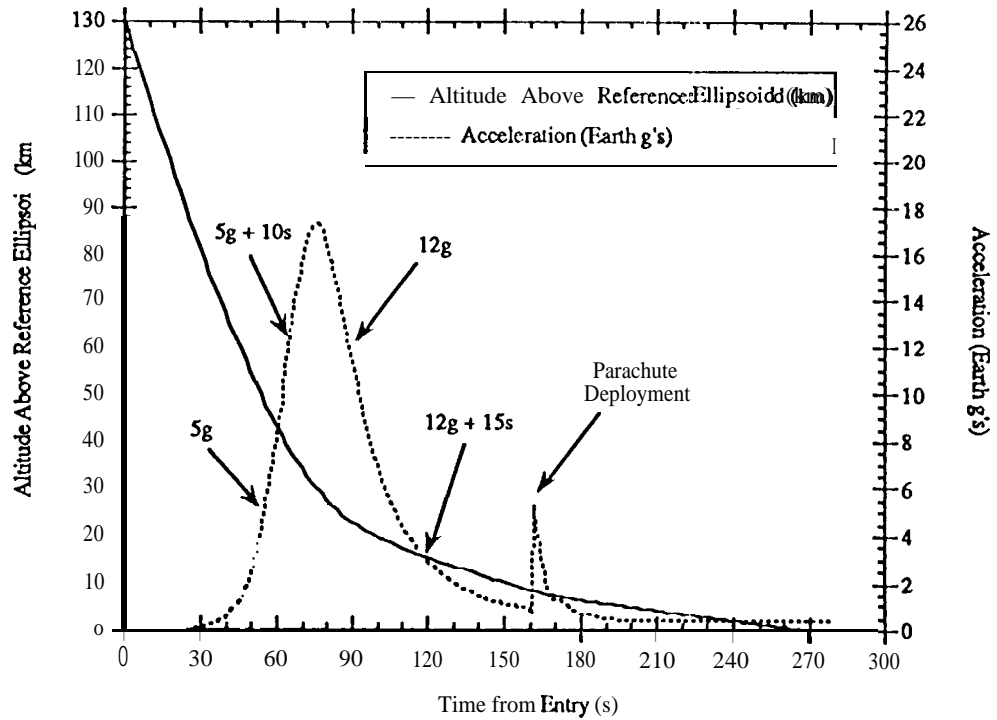


Figure 3. Altitude and Acceleration During Entry

ENTRY TRAJECTORY SIMULATION

Models

Atmosphere Model. The principal atmosphere model that has been used in the development of the Pathfinder entry trajectory is the Mars Global Reference Atmospheric Model (Mars-GRAM)⁹. Mars-GRAM includes mean density, temperature, pressure, and wind profiles, and statistical perturbation magnitudes for density variations. The model includes diurnal, seasonal, and positional (i.e., latitude and longitude) variations, as well as optional dust storm effects. Additional effects, such as solar flux and terrain-influenced atmospheric waves, are also available.

In the June 1994 Mars Pathfinder landing site selection workshop, the scientific community was in agreement that the Mars-GRAM atmosphere model was the most accurate model available. Since that time, Hubble Space Telescope observations and Earth-based microwave measurements¹⁰ have indicated that the atmosphere of Mars is significantly cooler and has a lower dust content than when it was observed by the Viking Landers. An atmosphere model (which will be referred to as the Clancy model) has been developed which is correlated to the more recent data. As seen in Figure 4, the Clancy model predicts atmospheric densities below the Mars-GRAM 3σ low density profile for altitudes between 30 km and 88 km. However, it has been demonstrated that the effects of the Clancy model on the Pathfinder entry trajectory are minimal. For the Pathfinder Monte Carlo simulations, atmospheric density uncertainties twice those computed in Mars-GRAM were used.

Entry Covariance Matrix. Initial conditions at the atmospheric interface point were generated by randomly sampling a covariance matrix¹¹, which was computed for the trajectory following the final Trajectory Correction Maneuver (TCM-4). The resulting inertial entry flight path angles have a 3σ variation of $\pm 10^\circ$ from the nominal value. The covariance matrix that was used in the Monte Carlo simulations is shown in Table 1. A complete definition of the covariance matrix and the associated variables is given in Reference 12.

Table 1. Post-TCM-4 Covariance Matrix

8.68487E+01	-2.98679E+01	9.47214E-01	6.21208E-06	-2.00968E-06	-3.15066E-05
-2.98679E+01	5.90933E+01	-8.51510E-01	-1.85256E-06	4.83299E-06	5.29953E-06
9.47214E-01	-8.51510E-01	4.52807E-01	6.36024E-08	3.90398E-08	2.47995E-05
6.21208E-06	-1.85256E-06	6.36024E-08	8.83108E-13	-1.35054E-13	-2.61029E-12
-2.00968E-06	4.83299E-06	3.90398E-08	-1.35054E-13	7.92739E-13	-5.13206E-13
-3.15066E-05	5.29953E-06	2.47995E-05	-2.61029E-12	-5.13206E-13	2.11270E-09

Gravity Field. The Monte Carlo simulation employs a simple gravity field with J_2 only, assuming a gravitational parameter for Mars of $42,828.28685 \text{ km}^3/\text{s}^2$, and a J_2 term of 0.0019628.

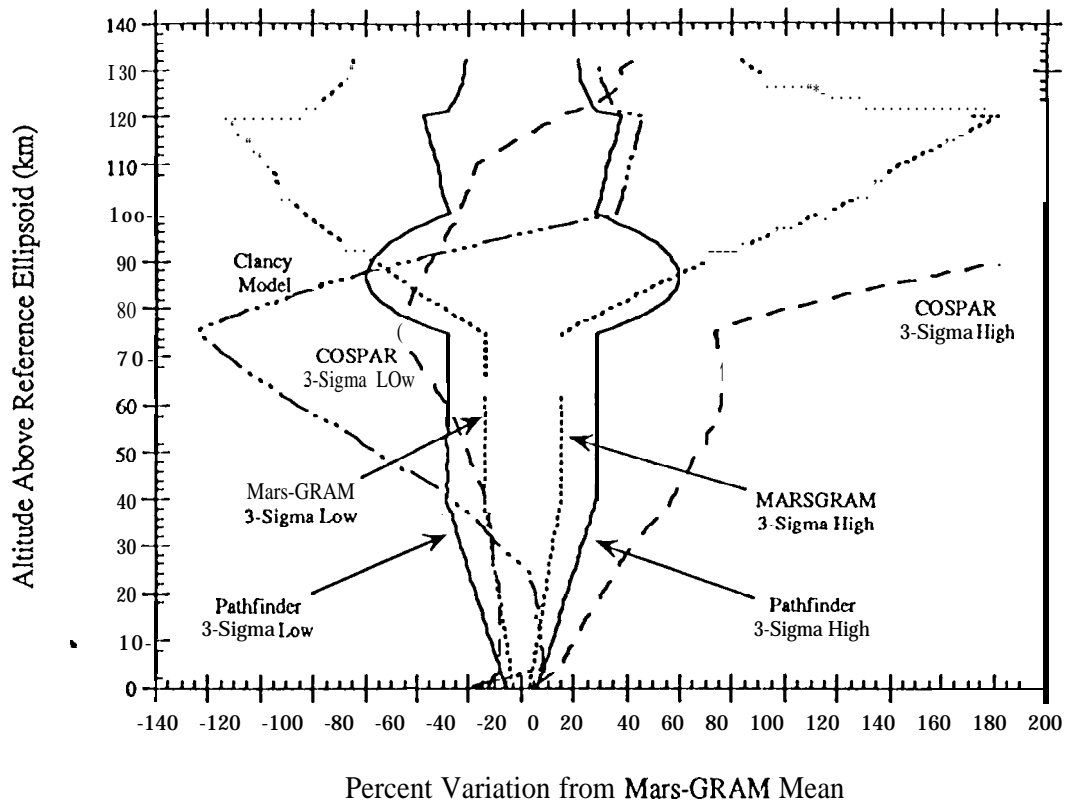


Figure 4. Mars Atmosphere Models Compared with Mars-GRAM Mean

Mass Properties. Worst-case mass properties for the entry vehicle were derived assuming a ballistic coefficient prior to peak heating of 65 kg/m^2 . The entry body mass properties are given in Table 2. The coordinate system for the mass properties, shown in Figure 5, has its origin located along the centerline of the vehicle, at the top of the cruise stage/entry vehicle interface pads. The +Z axis is directed along the spacecraft centerline, toward the tip of the conical aeroshell. The +Y axis is directed parallel to the Star Scanner, in the direction opposite interface bushing #1, and the +X axis completes the right-handed system.

Integrators. The 3 Degree-of-Freedom (DOF) and 6 DOF Monte Carlo simulations employ different numerical integrators. The 3 DOF Atmospheric Entry Program (AEP) uses a double precision variable order Adams predictor-corrector method¹³. A standard 4th order Runge-Kutta integration method¹⁴ was applied for the 6 DOF Program to Optimize Simulated Trajectories (POST) computations.

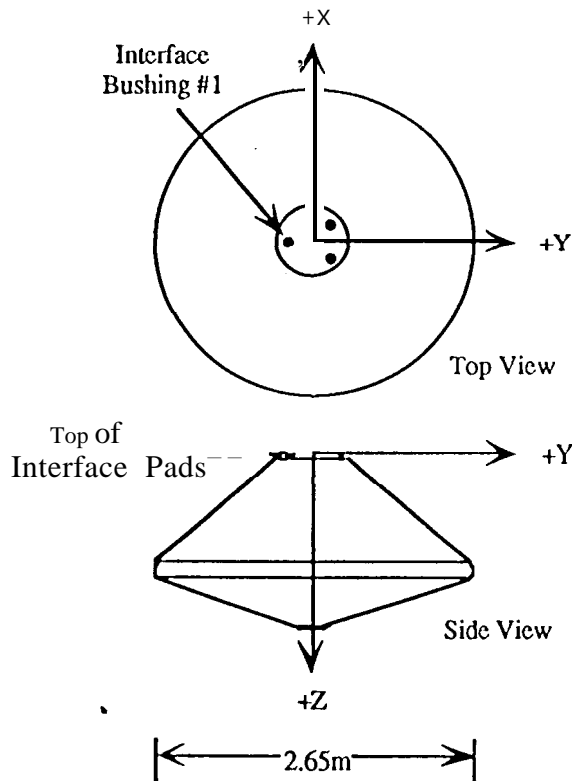


Figure 5. Entry Body Coordinate System

Table 2. Entry Body Mass Properties

Entry Mass: 905 kg

Center of Mass: $X = 0$ m
 $Y = 0$ m
 $Z = 0.818$ m

Inertia Properties:

$$I_{XX} = 196.5272 \text{ kg}\cdot\text{m}^2$$

$$I_{YY} = 201.7589 \text{ kg}\cdot\text{m}^2$$

$$I_{ZZ} = 248.5768 \text{ kg}\cdot\text{m}^2$$

$$I_{XY} = -1.1602 \text{ kg}\cdot\text{m}^2$$

$$I_{XZ} = -0.23599 \text{ kg}\cdot\text{m}^2$$

$$I_{YZ} = -0.57048 \text{ kg}\cdot\text{m}^2$$

Aerodynamics. An aerodynamic database was developed for use in the Monte Carlo analyses based on a combination of computational fluid dynamics calculations, wind-tunnel, and ballistic range test results. Proper estimation of the drag coefficient is **required** for the 3 DOF analysis, while the 6 DOF simulation requires three force coefficients as well as static and dynamic moment coefficients. Aerodynamic characteristics were obtained for the forebody of the Mars Pathfinder 70° sphere-cone **aeroshell** at numerous trajectory points (**from** entry interface to Mach 1.5), over an angle-of-attack range of 0° to 11°, with the High Alpha **Inviscid** Solution (**HALIS**)¹⁵, and the Langley **Aerothermodynamic** Upwind Relaxation Algorithm (**LAURA**) **codes**¹⁶. Base **effects** on drag coefficient were calculated by including the afterbody in several of the full-chemistry **Navier-Stokes** (**LAURA**) solutions. This computational data was supplemented by Viking test data^{17,18} and compared to the 110 angle-of-attack Viking flight data.

The 0° angle-of-attack drag coefficient profile is depicted in Figure **6**. The peak **aeroshell** drag coefficient is about 1.72. Three-sigma uncertainty levels for each aerodynamic coefficient were **estimated**²⁰. These subjective estimates were based on computational experience and comparison to similar entry configurations at similar **flowfield** conditions. For drag coefficient, an uncertainty of 2% was determined below Mach 10. Below Mach 5, the unsteady base **flowfield** has a greater impact, and there is less computational experience

with the LAURA code. A 3σ uncertainty on drag coefficient of 10% was used below Mach 5. Between Mach 5 and Mach 10, a linearly interpolated value for drag coefficient variation was used.

Both the computational solutions and the Viking ballistic range test data identify two low angle-of-attack static instability regions, at atmosphere-relative velocities of 6.5 km/s and 3.5 km/s. These static instability regions are discussed in detail in Reference 21. Experimental data produced in support of the Viking program also predicts the presence of a low angle-of-attack dynamic instability region below Mach 2.5. The impact of the three instability regions on the Pathfinder mission is discussed in Reference 22, and a thorough presentation of the Pathfinder aerodynamic data is provided in Reference 20.

Cruise Stage Separation. Based upon the current set of Pathfinder mass properties, a statistical cruise stage separation analysis predicts a 3s pointing error of 2.68° , a 3σ nutation of 4.36° , and a 3σ wobble of 1.97° at the atmospheric interface point. These predictions translate into a maximum of $\pm 9^\circ$ total angle-of-attack, and a maximum total attitude rate of $*1.50/s$ at the atmospheric interface point. These uncertainties were provided as input to the 6 DOF Monte Carlo analysis.

Nominal Entry Profile

The nominal trajectory for the Pathfinder entry vehicle has been designed based upon a worst-case entry mass of 603 kg, which corresponds to a ballistic coefficient of 65 kg/m^2 at peak heating (assuming $C_D = 1.68$). The arrival inertial velocity at the atmospheric interface point will vary depending upon the launch date, but will be within the range of 7.25 km/s to 7.35 km/s. For design purposes, the maximum entry velocity is used. It is noted that the arrival velocity increases with later launch dates, so an earlier launch date will result in additional margins. The nominal design entry state is given in Table 3, expressed in the Mars Mean Equator and Prime Meridian of Epoch coordinate frame¹².

A plot of altitude and acceleration versus time during entry for the nominal trajectory is shown in Figure 3. This trajectory reaches a maximum stagnation point pressure of 21.116 kPa, just prior to reaching the peak heating rate of 99 W/cm^2 . The maximum acceleration during entry is 17.3 Earth g's (169.5 m/s^2). The parachute is deployed at a dynamic pressure of 600 N/m^2 , at a Mach number of 2.10. Following the release of the heatshield, the terminal velocity of the system is 58 m/s, at an altitude of 50 m above the assumed ground level (the nominal landing site elevation is 0.60 km below the Mars reference ellipsoid). The total integrated stagnation point heat load during the descent is 3608 J/cm^* .

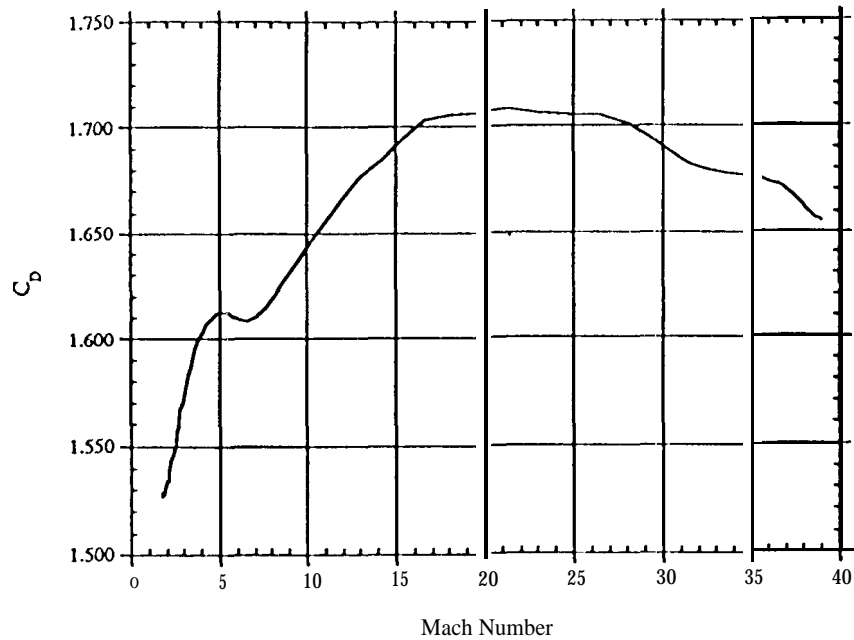


Figure 6. Pathfinder Nominal C_D Profile

Table 3. Nominal Mars Atmospheric Entry State

Entry Date and Time (UTC)	7/4/97 16:46:34
Radius (km)	3522.2000
Latitude (deg)	22.9840
Longitude (deg)	338.9036
Velocity (km/s)	7.3509
Flight Path Angle (deg)	-14.2000
Flight Path Azimuth (deg)	253.0995

Throughout the entry portion of the flight, vehicle spin and aerodynamic damping are relied upon to provide vehicle stability about the nominal 0° trim angle of attack. The entry vehicle will enter the atmosphere with a nominal 2 rpm roll rate. Six DOF trajectory analysis has shown that the Mars Pathfinder **aeroshell** is aerodynamically stable over a large portion of the atmospheric flight. However, two low angle of attack static instabilities (hypersonic) and a low angle of attack dynamic instability (supersonic) have been identified and shown to cause an increase in vehicle angle of attack away from the trim state. In each of these flight regimes, the vehicle is aerodynamically stable at higher angles of attack, such that the increase in vehicle angle of attack is bounded. The nominal attitude profile is shown in Figure 7. In general, this attitude motion is characterized by: an increase in vehicle angle of attack just prior to peak heating; flight with a lower angle of attack, but higher oscillation frequency through peak dynamic pressure; a second increase in vehicle angle of attack just prior to peak Reynolds number, which is quickly damped; a final increase in vehicle angle of attack as parachute deployment is reached,

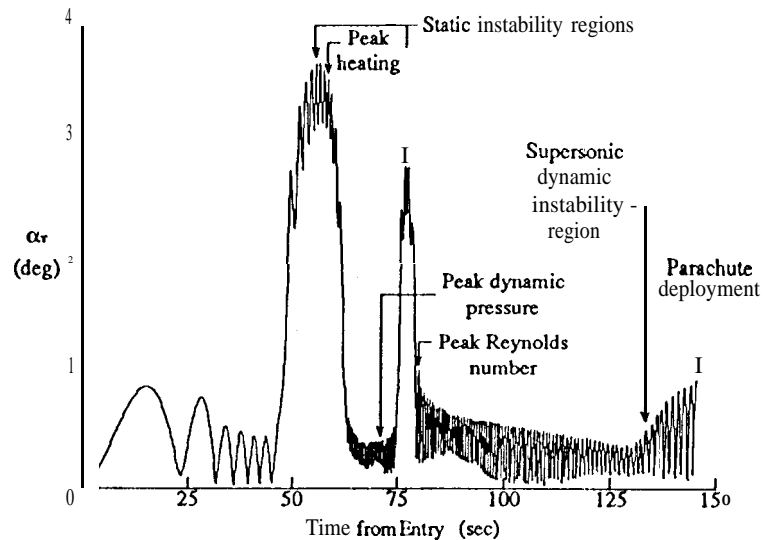


Figure 7. Nominal 6 DOF Total Angle of Attack Profile

Monte Carlo Simulation and Statistical Analysis

While computationally intensive, the Monte Carlo approach can give insight into the behavior of systems that are too complex to be resolved analytically. Three DOF (translational) and 6 DOF (translational and rotational) Monte Carlo simulations have been developed, to obtain statistical information on conditions at critical points during the Pathfinder descent. The 6 DOF simulation is more complete in its representation of the entry body aerodynamics, and the 6 DOF results are used for the verification of EDL system requirements. The 3 DOF simulation is useful for modelling the terminal descent phase of the trajectory, following parachute deployment, and, as an independent simulation, the 3 DOF simulation provides a useful check of the 6 DOF results.

Table 4 contains the variables for the 3 DOF Monte Carlo simulations. The perturbed initial entry state is determined by post-multiplying the Cholesky factor of the 6 x 6 covariance matrix (Table 1) with a 6 x 1 random vector, with each element in the random vector having zero mean and unit variance, and adding the resulting vector to the nominal entry state. The atmospheric density profile is determined by two randomly generated scale factors, for the upper (above 100 km) and lower (below 75 km) atmosphere. Between 75 km and 100 km, the scale factor is linearly interpolated from the upper and lower altitude scale factors. The scale factors are multiplied by the Mars-GRAM density standard deviation, and the resulting density perturbations are added to the Mars-GRAM mean density profile. While this approach for generating density profiles does not necessarily result in profiles that are physically realizable, it bounds the likely profiles and produces meaningful statistical results when used in a Monte Carlo simulation. The dispersions on event timing and accelerometer measurements shown in Table 4 are applied to the parachute deployment algorithm. The 6 DOF Monte Carlo simulation includes additional uncertainties on aerodynamic coefficients, entry body center of gravity location, and initial attitude and attitude rates. The nominal

values and 3σ variations for the 6 DOF Monte Carlo simulation are given in Reference 22.

Table 4. Three DOF Monte Carlo Simulation Variables

Input Variable	Nominal	Variation	Distribution
Initial Entry State	See Table 3	Based upon Covariance Matrix See Table 1	Normal
Atmospheric Density	Mars-GRAM Mean	Mars-GRAM $\pm 6\sigma$ Below 75 km Mars-GRAM $\pm 1\sigma$ Above 100 km Linearly Interpolate between 75-km and 100 km	Normal
Entry Body Drag Coefficient	See Figure 6	$\pm 2\%$ (3σ) Mach ≥ 10 $\pm 10\%$ (3σ) Mach ≤ 5 Interpolate for $5 < \text{Mach} < 10$	Normal
Parachute Drag Coefficient	Viking Drag Profile	$\pm 13\%$ (3σ)	Normal
Accelerometer Error	0.0 m/s ²	± 4.9 m/s ² (3σ)	Normal
Event Timing Error	0.0 s	± 0.25 s (3σ)	Normal
Landing Site Elevation	-0.60 km	± 1.0 km (3σ)	Normal

Results from the 3 DOF and 6 DOF Monte Carlo simulations are shown in Table 5. For both simulations, 2000 cases were run. Trajectory and attitude conditions are given at critical points during atmospheric entry, in terms of the statistical mean, standard deviation, and 3σ range. Altitudes in Table 5 are given with respect to the Mars reference ellipsoid. The variable α_r represents total angle-of-attack, and γ represents flight path angle. Note that velocity and flight path angle are given with respect to an atmosphere-relative coordinate frame.

The 6 DOF simulation terminates at the time of parachute deployment. The 6 DOF conditions at parachute deployment were passed into the 3 DOF simulation, so that values could be obtained at the times of **heatshield** release, bridle deployment, and Rocket Assisted Deceleration (**RAD**) firing. A complete multi-body (parachute, **backshell**, and lander) simulation for the terminal descent phase of the entry trajectory is in development at the Jet Propulsion Laboratory Mechanical Systems Engineering and Research Division²³.

In general, there is excellent agreement between the 3 DOF and 6 DOF simulations, on the mean values of the trajectory conditions at the various EDL events. However, it is seen that the standard deviations for the 6 DOF results are consistently larger than those for the 3 DOF data. This greater variation is due to the aerodynamic effects accounted for in the 6 DOF simulation, namely, a variation in the **drag coefficient** due to a changing angle-of-attack, as well as lift effects.

A histogram of total angle-of-attack at peak heating (computed in the 6 DOF simulation) is shown in Figure 8. Figure 9 shows a scatter plot of the 6 DOF altitude and dynamic pressure at the time of parachute deployment. The 3 DOF landing ellipse on the Mars surface is shown in Figure 10.

Table 5. 3 DOF and 6 DOF Monte Carlo Simulation Results

Event	3 DOF Mean Value	3 DOF Standard Deviation	3 DOF 3σ Range	6 DOF Mean Value	6 DOF Standard Deviation	6 DOF 3σ Range
Peak Heat Rate (W/cm^2)	98.57	2.45	91.21—105.92	†	†	†
Peak Heating α_r (deg)	*	*	*	4.88	0.53	3.29—6.47
Peak Acceleration (Earth g's)	169.62	9.42	141.37—197.88	†	†	†
Max Stagnation Point Temperature (K)	21.101	1.182	17.555—24.647	†	†	†
Parachute Deployment						
Time from Entry (sec)	162.70	9.58	133.97—191.44	162.93	8.81	136.50—189.36
Altitude (km)	8.01	0.80	5.63—10.40	7.94	1.16	4.46—11.42
V_a (kn/sec)	0.386	0.015	0.340—0.431	0.386	0.026	0.308—0.464
γ (deg)	-25.83	0.90	-28.53—23.12	-25.93	1.81	-31.36—20.50
α_r (deg)	*	*	*	1.77	0.76	0.00—4.05
Acceleration (Earth g's)	*	*	*	0.833	0.044	0.701—0.965
Mach Number	1.72	0.07	1.51—1.94	1.72	0.12	1.36—2.08
Dynamic Pressure (N/m^2)	585.9	35.0	480.87—691.0	586.1	39.1	468.8—703.4
Heatshield Release						
Time from Entry (sec)	182.70	9.58	153.97—211.44	182.93	8.81	156.50—209.36
Altitude (km)	5.92	0.77	3.60—8.25	5.85	1.13	2.464—8.24
V_a (km/sec)	0.110	0.006	0.093—0.127	0.111	0.014	0.070—0.151
γ (deg)	-45.65	1.39	-49.83—-41.48	-45.76	2.95	-54.60—-36.91
Acceleration (Earth g's)	0.729	0.029	0.643—0.815	0.734	0.066	0.5374—0.931
Mach Number	0.49	0.03	0.41—0.56	0.49	0.06	0.31—0.67
Dynamic Pressure (N/m^2)	57.1	4.2	44.4—69.7	58.8	12.9	20.1—97.6
Total Integrated Heating (J/cm^2)	3615	89	3348—3881	t	t	t
Bridle Fully Deployed						
Time from Entry (sec)	207.70	9.58	178.97—236.44	207.93	8.81	181.50—234.36
Altitude (km)				4.02	1.09	0.75—7.30
V_a (kn/sec)				0.0075	0.006	0.057—0.092
γ (deg)				-7.4662	2.61	-82.43—-66.80
Acceleration (Earth g's)				0.397	0.005	0.381—0.413
Mach Number				0.33	0.03	0.254—0.41
Dynamic Pressure (N/m^2)				31.6	4.8	17.3—45.9
Ground Acquisition (1500 m AGL)						
Time from Chute Deploy (sec)	92.23			90.95	16.82	40.50—141.40
RAD Firing						
Time from Entry (sec)				276.78	20.78	214.43—339.12
Altitude (km)				-0.487	0.327	-1.469—0.493
V_a (km/sec)				0.058	0.004	0.045—0.071
γ (deg)				-89.56	0.60	-90.00—-87.74
Acceleration (Earth g's)				0.399	0.003	0.389—0.408
Mach Number				0.26	0.02	0.20—0.32
Dynamic Pressure (N/m^2)				31.7	4.6	17.9—45.5

THESE BOXES
WILL BE
FILLED IN

* Computed in 6 DOF simulation only.

† Computed in 3 DOF simulation only.

The Monte Carlo simulation results indicate that the required conditions at parachute deployment are met by the 3σ range of trajectories. The range of total integrated heating, and the dynamic pressures at heatshield release, are within the limits of the aeroshell design. The EDL System requirement of 55 seconds from parachute deployment to 1500 m altitude (AGL) is met in 2.10 (95%) of the 6 DOF trajectories. This is an acceptable risk level to the

Pathfinder Project, as recent design improvements in the bridle subsystem have increased the margin in the terminal descent timeline.

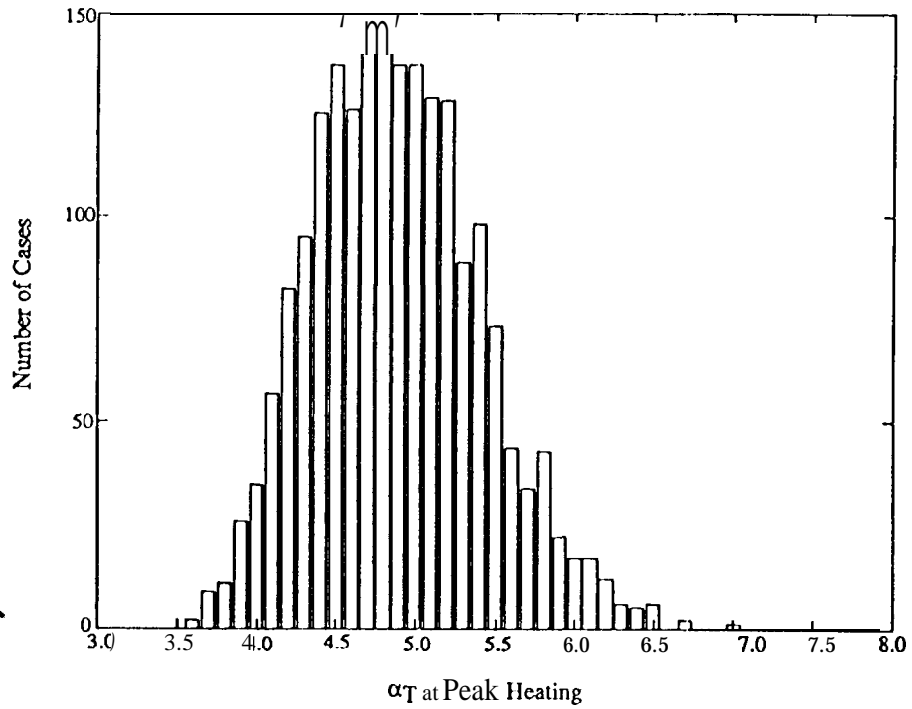


Figure 8. 6 DOF Histogram, Total Angle-of-Attack at Peak Heating

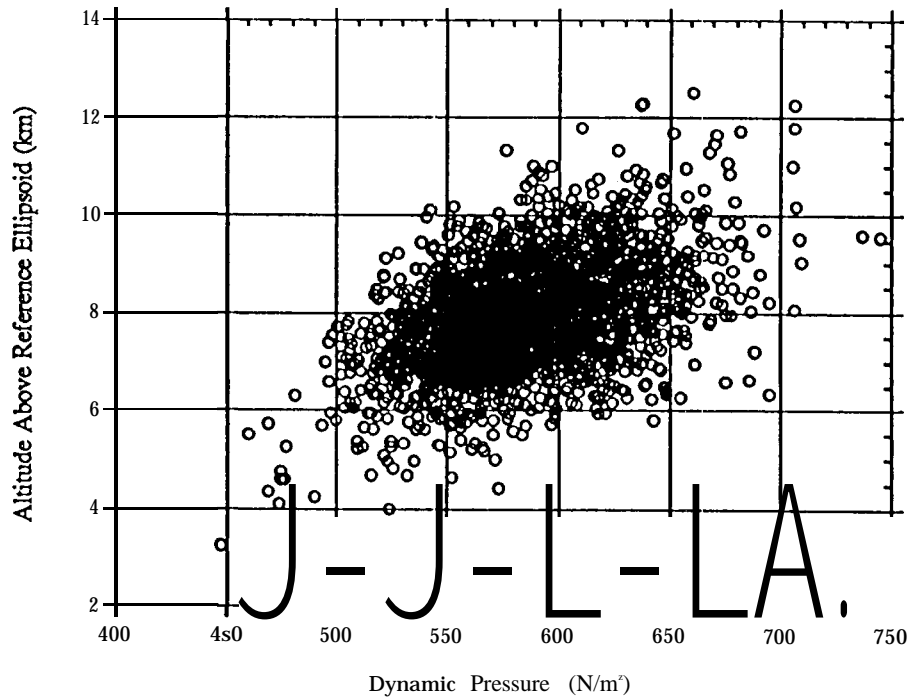


Figure 9. 6 DOF Altitude and Dynamic Pressure at Parachute Deployment

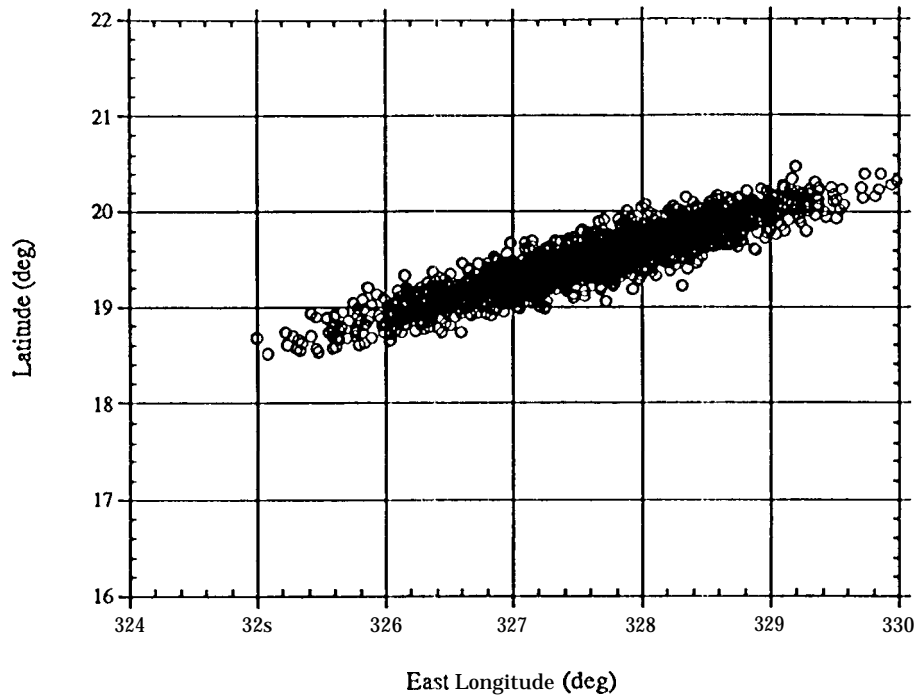


Figure 10. 3 DOF Landing Ellipse

CONCLUSION

Design of the Pathfinder entry trajectory, and identification of the likely trajectory dispersions during critical events, have been essential for the development of the various EDL subsystems. Monte Carlo simulations have been instrumental in quantifying the statistical uncertainties associated with trajectory and attitude conditions during the atmospheric entry. In general, the 6 DOF simulation results are used to determine the 3σ bounds on trajectory and attitude conditions during entry, up to the time of parachute deployment. The 3 DOF simulation is useful for preliminary trade studies, and simulation of the terminal descent (after parachute deployment). In addition, the 3 DOF simulation provides a useful check of the 6 DOF results.

The Pathfinder entry trajectory **design currently** meets all EDL requirements with a significant amount of margin, providing a high level of confidence that Pathfinder's **five** minutes of flight through the Mars atmosphere will result in a successful landing.

ACKNOWLEDGMENTS

The authors would like to acknowledge the contributions of several individuals to this work. Richard Cook was responsible for the Mars Pathfinder interplanetary trajectory design, and the early atmospheric entry trajectory design. Gurkirpal Singh contributed to the design of the parachute deployment algorithm. Pieter Kallemeyn provided the entry covariance matrix. Walt Engelund, Peter Gnoffo, Bob Mitcheltree, and James Weilmuenster developed the entry body aerodynamics database.

REFERENCES

1. W. M. Congdon, "Ablation Model Validation and Analytical Sensitivity Study for the Mars Pathfinder Heat Shield," AIAA 95-2129, 30th AIAA Thermophysics Conference, San Diego, CA, June 19-22, 1995.
2. "Mars Pathfinder Navigation Plan Critical Design Review Version," JPL-D 11349, Jet Propulsion Laboratory, California Institute of Technology, July 1994.
3. R. A. Cook and J.B. McNamee, "Mission Design for the Mars Environmental Survey," AAS 93-563, AAS/AIAA Astrodynamics Specialist Conference, Victoria, B. C., Canada, August 16-19, 1993.
4. A. Seiff, "Mars Atmospheric Winds Indicated by Motion of the Viking Landers During Parachute Descent," *J. of Geophys. Res.*, Vol. 98, No. E4, pp. 7461-7474, April 25, 1993.
5. M. Golombek, et al, "Mars Pathfinder Landing Site Workshop," Lunar and Planetary Institute Tech. Report No. 94-04, April 1994.
6. M. Tauber, et al, "Ames Research Center Mars/Pathfinder Heat Shield Design Verification Arc-Jet Tests," March 15, 1995.
7. "Mars Pathfinder Parachute Decelerator Subsystem Performance Requirements Specifications," JPL Contract No. 960078, Exhibit III, 6 January, 1995.
8. G. Singh, "Mars Pathfinder Accelerometer Algorithm," JPL D-12532, Jet Propulsion Laboratory, California Institute of Technology, March 17, 1995.
9. C. G. Justus and G. Chimonas, "The Mars Global Reference Atmospheric Model (Mars-GRAM)," Technical Report, Georgia Tech Project G-35-685, Prepared for NASA Marshall Space Flight Center under Grant No. NAG8-078, July, 1989.
10. R. T. Clancy, et al, "A New Model of Mars Atmospheric Dust Based Upon Analysis of Ultraviolet through Infrared Observations from Mariner-9, Viking, and Phobos," *J. Geophys. Res.*, Vol. 100, pp. 5251-5263, 1995.
11. T. D. Moyer, "Mathematical Formulation of the Double-Precision Orbit Determination Program (DPODP)," Tech. Report 32-1527, Jet Propulsion Laboratory, California Institute of Technology, May 15, 1971.
12. "Mars Pathfinder Planetary Constants and Models Document," In Preparation, Jet Propulsion Laboratory, August 1995.

13. F. T. Krogh, et al, "MATH77 and mathc90, Release 5.0, Libraries of Mathematical Subprograms in FORTRAN 77 and C," JPL D-1 341, Rev. D, January 1995.
14. G.L. Brauer, et al, "Capabilities and Applications of the Program to Optimize Simulated Trajectories (POST)," NASA CR-2770, February 1977.
15. K.J. Weilmuenster and H.H. Hamilton, II, "Computed and Experimental Surface Pressure and Heating on 70-Deg Sphere Cones," *J. Spacecraft and Rockets*, Vol. 24, No. 5, September-October 1987, pp. 385-393.
16. P.A. Gnoffo, "Upwind-Biased, Point-Implicit Relaxation Strategies for Viscous, Hypersonic Flows," AIAA 89-1972, June 1989.
17. "Viking Aerodynamics Data Book," TR-3709014, Prepared under Contract No. NAS 1-9000, Martin Marietta Corporation, Denver, Colorado, June 1972.
18. "Experimental Pitch Damping Derivatives for Candidate Viking Entry Configurations at Mach Numbers from 0.6-3.0," TR-3709005, Prepared under Contract No. NAS 1-9000, Martin Marietta Corporation, Denver, Colorado, June 1970.
19. B.L. Uselton, et al, "Damping-in-Pitch Derivatives of 120- and 140-deg Blunted Cones at Mach Numbers from 0.6 through 3.0," AEDC-TR-70-49, April 1970.
20. W.C. Engelund, et al, "Aerodynamic Characteristics of the Mars Pathfinder Atmospheric Entry Configuration," To be Released as a NASA TM, August 1995.
21. P.A. Gnoffo, et al, "Effect of Sonic Line Transition on Aerothermodynamics of the MESUR Pathfinder Probe," AIAA 95-1825, 13th AIAA Applied Aerodynamics Conference, San Diego, California, June 19-22, 1995.
22. R.D. Braun, et al, "Mars Pathfinder Six Degree of Freedom Entry Analysis," To be Published in the *J. of Spacecraft and Rockets*, 1995.
23. K.S. Smith, et al, "Multibody Dynamic Simulation of Mars Pathfinder Entry, Descent, and Landing," Document in Preparation, Jet Propulsion Laboratory, Pasadena, California, August 1995.